Desalination and Water Treatment
www.deswater.com

doi: 10.5004/dwt.2020.25711

191 (2020) 164–172
July

Modified strawberry calyx as an efficient adsorbent for Ni(II) ions adsorption: a central composite design approach for multivariate sorption optimization

Adnan Ahmed[a], Ali Nawaz Siyal[b,*], Sumita Bhatia[a], Saima Qayoom Memon[b], Amanullah Mahar[a]

[a]*Centre for Environmental Science, University of Sindh, Jamshoro 76080, Pakistan, Tel. +92 333 2891399; email: adnan.jaat@gmail.com (A. Ahmed), Tel. +92 3313549716; email: deepabhatia399@gmail.com (S. Bhatia), Tel. +92 33061971794; email: aman.fsw@gmail.com (A. Mahar)*

[b]*Institute of Chemistry, University of Sindh, Jamshoro 76080, Pakistan, Tel. +92 22 921311 Ext. 2004; emails: alinsiyal@usindh.edu.pk (A.N. Siyal), msaima77@gmail.com/saimaqmemon@usindh.edu.pk (S.Q. Memon)*

Received 1 September 2019; Accepted 16 February 2020

ABSTRACT

In this study, strawberry calyx waste was converted to efficient adsorbent by treating with 0.5 mol L^{-1} HCl for the uptake of Ni(II) ions from environmental aqueous samples. Multivariate sorption optimization was carried out by the central composite design model, contained 18 experiments. Removal of Ni(II) ions was achieved 98.5% with relative standard deviation (RSD) ≤ 3.5% at optimum pH 8.0, sorbent dose 70 mg, concentration of Ni(II) ions 50 mg L^{-1}, shaking speed 100 rpm and shaking time 95 min at temperature 25°C. The different interactive effects of two factors on the response were studied simultaneously. Analysis of variance reveals that the numerical value of P is ≤ 0.05 for all effects except the effect of adsorbent dosage and shaking time which indicated that all the null hypotheses are rejected except the interactive effect of adsorbent dosage and shaking time. Langmuir and Dubinin–Radushkevich isotherms fitted well to adsorption data with correlation coefficient (R^2) of 0.995 and 0.989, respectively. Monolayer sorption capacity of adsorbent for the uptake of Ni(II) ions was found to be 45.3 ± 2.4 mg g^{-1}. The sorption energy was found to be 14.81 ± 1.5 kJ mol^{-1} which indicated that Ni(II) ions were adsorbed onto the adsorbent by chemisorption or ion exchange mechanism. The method was applied on real environmental aqueous samples for the removal of Ni(II) ions.

Keywords: Strawberry; Calyx waste; Removal; Ni(II) ions; Adsorption; Equilibrium; CCD model

---

1. Introduction

Water is the most essential for the survival of living organisms. The availability of clean water for humans has become a global crisis due to its continuous contamination and population growth [1,2]. About 71% of earth's surface is covered with water. About 97.3% of total water is present in oceans and only 2.7% is drinkable. About 2.04% of drinkable water is found in glaciers and ice caps, 0.61% is present as groundwater. About 1,02,960.58 billion acre-feet (1.0 acre-foot = 435,600 cubic feet) is present in rivers, lakes and other sources [3]. Approximately 33% of people in the world are consuming water from underground sources for drinking [4]. About 1,200 million people do not have excess to clean water and about 2,600 million people do not have fundamental sanitation facilities [5]. According to WHO, about 1.6 million people die annually due to water-borne diseases such as diarrhea, and about 90% of these deaths are in children under the age of 5 y [6]. Rapid growth in industrialization, modernization, growing civilizations, growing populations, agricultural pesticides, and insecticides, geological changes and other environmental issues have been causing water contamination [7]. The discharge

---

* Corresponding author.

of metallic contaminated industrial effluents into environmental aqueous bodies is a potential threat to humans, animals, and plants due to its non-biodegradable nature unlike the organic pollutants [8,9]. Excess intake of toxic metal ions through the food chain and/or other means causes serious health problems by interacting with nitrogen, sulfur and oxygen of proteins and replacement of metal ions from certain enzymes resulting in malfunctioning or cells destroying [10]. In developed countries, it is legislated that the metal-contaminated industrial effluents must be treated prior to their discharge into water bodies [11]. Industrial effluent discharge causes Ni(II) ions contamination in environmental aquatic bodies. According to the United States Environmental Protection Agency, the maximum allowable concentration of Ni(II) ions in drinking water is 0.1 mg L^{-1} [12], exceeding this limit, it causes health problems such as gastrointestinal distress, restlessness, nausea, vomiting, migraine, chest tightness, chest pain, breathlessness, hacking cough, shortness of breath, weakness, cyanosis dermatitis, fibrosis and some carcinogenic diseases including kidney failure and cancers in lungs, nose, and bones [13,14]. Several methods based on coagulation, co-precipitation, ion exchange, reverse osmosis, solvent extraction, and adsorption have been developed for water treatment [15]. Among these, adsorption is the most recommended in physicochemical technologies because of least solvent consumption, cost-effective, operational ease, reusability of adsorbents and high efficiency of adsorbents for adsorbate [16]. Agricultural based materials contain cellulose and lignin which comprise of a different functional group such as aldehydes, alcohols, ketones, carboxylic acids, ether, and phenols. Agricultural waste-based adsorbent containing hydroxyl and carboxyl groups, which have a strong ability to bind with metal ions [17]. For the last decades, the agricultural waste-based adsorbents have been widely used for the adsorption of metal ions because of their low cost and containing polar functional groups. The literature review confirmed strawberry calyx of strawberry fruit has not been used for the synthesis of the adsorbent. In this study, we focus to convert strawberry calyx waste to efficient adsorbent by treating with hydrochloric acid for Ni(II) ions uptake from environmental water samples. Central composite design (CCD) will be employed for multivariate sorption optimization.

2. Experimental setup

2.1. Material

PerkinElmer flame atomic spectrometer (AAnalyst 800, USA) equipped with hollow cathode lamp was employed for the determination of Ni(II) ions. Thermo Scientific Fourier-transform infrared (FT-IR) spectrometer (Nicolet iS10, UK) was used for recording the FT-IR spectrum. An automatic temperature-controlled digital shaker (Model No.1-4000, Germany) was used for shaking purposes. For pH measurements, pH meter (inoLab pH 720, Germany) was used. Double distilled water and analytical reagent grade chemicals were used throughout the research. $Ni(NO_3)_2·6H_2O$, HCl, CH_3COOH, CH_3COONa, H_3PO_4, NaH_2PO_4, NH_4OH, and NH_4Cl were purchased from Sigma-Aldrich, China. CH_3COOH/CH_3COONa, H_3PO_4/NaH_2PO_4, and NH_4OH/NH_4Cl were used as buffer solutions for the adjusting of pH. STATGRAPHICS (Statpoint Technologies Inc., version 16.1.11, 32 bit, USA) was used for statistical analysis.

2.2. Water samples collection

Pre-washed glass bottles were used for wastewater samples collection from combined effluent treatment plant (CETP) in Korangi, Karachi on 8th February 2019 at 11.20 am. The samples were filtered through Whatman filter paper (pore size 2.5 μm) and stored into the refrigerator at 4.0°C.

2.3. Strawberry fruit

The botanical name of strawberry fruit is *Fragaria x ananassa*. The letter *x* between two names shows a hybrid breed of plant, which belongs to the kingdom *Plantae* and subkingdom *Tracheobionta*. The super division of this plant species is *Spermatophyta*. The class is *Magnoliopsida* and the subclass is *Rosidae*, which means that this is a hybrid of berry and rose family. The order of this plant is *Rosales* and belonging family is *Rosaceae* and Genus is *Fragaria L.* [18].

2.4. Preparation of adsorbent

Strawberry fruit is mainly attracted by the people for good taste, nutrition, aroma and its widespread uses in baking, fresh juices, and smoothies. The calyx is the leaf cap of strawberry fruit which was collected from fresh juice shops in the local market, Hyderabad, Sindh, Pakistan in February 2018. The calyx was washed with water, air-dried for 96 h, cut to small pieces and oven-dried at 60°C for 48 h. The material was ground by mortar and pestle and again oven-dried at 80°C for 96 h. Thereafter, the material was passed through a sieve (0.025 mm) and used for further treatment.

2.5. Activation of adsorbent

The adsorbent was washing repeatedly with water until the filtrate became transparent. Thereafter, 5.0 g of dried material was placed into a 500 ml conical flask containing 250 mL of 0.5 mol L^{-1} HCl and stirred at 200 rpm for 24 h. The mixture was filtered, subsequently washed with water and dilute solution of Na_2CO_3 until the filtrate became neutral and oven-dried at 80°C for a period of 96 h. The material was subjected to the FT-IR Spectrometer for characterization and applied as an adsorbent for solid-phase extractive uptake of Ni(II) ions from aqueous samples.

2.6. Variables

The response is dependent variable and factors are independent variables. The response changes with change in a factor. In adsorption study, adsorption (%) or removal (%) is response while factors may be adsorbent dose (*A*), initial concentration of Ni(II) ions (*B*), pH of the solution (*C*), and shaking time (*D*) [19]. The factors were fixed at three levels such as minimum level coded as a negative sign (–), intermediate level coded as zero (0) and the maximum level coded as a positive sign (+), respectively. For multivariate sorption optimization of Ni(II) ions, the factors and their levels are summarized in Table 1.

2.7. CCD model and adsorption experiments

For multivariate sorption optimization of Ni(II) ions, the CCD model with n^k design was chosen. The n^k design with four factors ($k = 4$) and two levels ($n = 2$) contains sixteen number of experiments (runs) with two replicates (center points) experiments were formulated. For multivariate sorption optimization of Ni(II) ions, 18 batch experiments at different levels of factors are summarized in Table 2. Statistically, the removal (%) of Ni(II) ions was predicted by the model for 18 experiments as given in Table 2. Eighteen batch experiments were performed and results are summarized in Table 2. The predicted and experimental removals were found in good agreement with $R^2 = 99.96\%$, which indicated that the CCD model fitted well to the experimental data.

2.8. Sorption experiment at optimum conditions

The efficiency of adsorbent and fitness of the model was checked by performing adsorption experiments at optimum conditions as predicted by the CCD model. Experimentally, 20 ml of 50 mg L^{-1} of Ni(II) solution of pH 8 was placed into 50 mL of the conical flask containing 70 mg of the adsorbent. The mixture was agitated with 100 rpm for 95 min at 25°C. The mixture was filtered and filtrated and subjected to the flame atomic absorption spectrometer for the determination of final concentration (C_e) of Ni(II) ions. The removal (%) of Ni(II) ions was achieved 98.5% with relative standard deviation (RSD) ≤ 3.5% as calculated by Eq. (1).

$$\text{Removal}\left(\%\right) = \frac{C_i - C_e}{C_i} \times 100 \tag{1}$$

where C_i and C_e are concentrations of Ni(II) ions at initial and equilibrium stages, respectively.

Table 1
Three levels of factors for multivariate sorption optimization of Ni(II) ions

Factor	Levels of factors		
	Minimum (–1)	Intermediate (0)	Maximum (+1)
A	10	55.0	100
B	10	55.0	100
C	2.0	05.5	9.0
D	10	95.0	180

Table 2
CCD model of n^k design and adsorption experiments for multivariate sorption optimization of Ni(II) ions

Run	Dose (mg)	pH	Concentration (mg L^{-1})	Time (min)	Removal (%)	
					Experimental	Predicted
1	1	–1	1	1	40.59	40.46
2	0	0	1	0	72.94	73.45
3	1	1	1	–1	80.42	80.29
4	–1	–1	1	–1	43.96	43.82
5	–1	0	0	0	35.56	35.33
6	0	0	0	0	59.19	60.43
7	–1	1	1	1	64.55	64.41
8	0	–1	0	0	56.30	56.06
9	0	0	–1	0	49.14	48.17
10	1	–1	–1	1	5.04	5.29
11	1	1	–1	–1	80.67	80.92
12	0	0	0	1	51.26	51.03
13	–1	1	–1	1	31.93	32.18
14	0	0	0	–1	39.50	39.26
15	0	1	0	0	96.33	96.10
16	1	0	0	0	52.64	52.40
17	0	0	0	0	60.27	60.43
18	–1	–1	–1	–1	9.24	9.50

3. Results and discussion

3.1. Characterizations of adsorbent

Fig. 1 shows the FT-IR spectrum of activated (acid-treated) material. The characteristic peaks at 3,326.37; 2,918.69; 1,732.40; 1,605.42; and 1,020.37 cm^{-1} correspond to stretching vibrations of O–H bond of alcohol, Sp^{3}C–H bond of the alkyl group, O=C bond of carbonyl, N=C bond of imine and C–N bond of amine moieties, respectively. This spectral information reveals that adsorbent is rich of polar functional groups. The hydroxyl (–OH) groups of alcohol and carboxylic acid can bind with metal ions.

3.2. Interactive effect of two factors on response

3.2.1. Effect of pH and concentration

Fig. 2 is the three dimensional (3D) plot, which depicts the interactive effect of pH ranging 2–9.0 and concentration of Ni(II) ions ranging 10–100 mg L^{-1} on the removal of Ni(II) ions at an optimum level of adsorbent dose 70 mg and shaking time 95 min. The result shows that the removal was not significantly influenced by pH 2–5, but increased significantly with the increase in pH 5–9. This effect of pH is explained as adsorbent became negatively charged by the release of proton in basic medium, which interacted with positively charged Ni(II) ions as it exists as main species at pH 8. The removal was also increased with an increase in the concentration of Ni(II) ions as more active sites are remained available onto the surface of the adsorbent for the retention of Ni(II) ions.

3.2.2. Effect of pH and sorbent dose

Fig. 3 depicts the interactive effect of pH ranging 2–9 and adsorbent dosage ranging 10–100 mg on the removal of Ni(II) ions at an optimum level of concentration 50 mg L^{-1} and shaking time 95 min. The result shows that removal was remained almost constant at an adsorbent dosage of 10–50 mg and decreased with further increase in adsorbent dosage, while the removal was increased significantly with increasing of pH as adsorbent became negatively charged by the release of proton in basic medium, which interacted with positively charged Ni(II) ions during adsorption.

3.2.3. Effect of pH and shaking time

Fig. 4 depicts the interactive effect of pH ranging from 2 to 9 and shaking time from 10–180 min on the removal of Ni(II) ions at the optimum level of concentration 50 mg L^{-1} and adsorbent dosage of 70 mg. The result shows that adsorption was increased with the increase of shaking time became maximum at 90 min as system attained the equilibrium at this stage, and slightly decreased with further increase in shaking time due to the desorption, while pH has the almost same effect as discussed in subsection 3.2.1.

3.2.4. Effect of shaking time and sorbent dose

Fig. 5 shows the interactive effect of adsorbent dose ranging from 10–100 and shaking time ranging from 10–180 min on the removal of Ni(II) ions at an optimum level of pH 8 and concentration 50 mg L^{-1} The removal was slightly increased with increased in adsorbent dose 10–50 mg, remained constant with further increase in adsorbent dose from 50–70 mg as system attained the equilibrium, and slightly decreased with further increase. In adsorbent dose, while shaking time has almost same effect as discussed in subsection 3.2.3.

3.2.5. Effect of concentration and adsorbent dose

Fig. 6 shows the interactive effect of concentration ranging from 10–100 mg L^{-1} and adsorbent dose ranging from 10–100 mg on the removal of Ni(II) ions at the

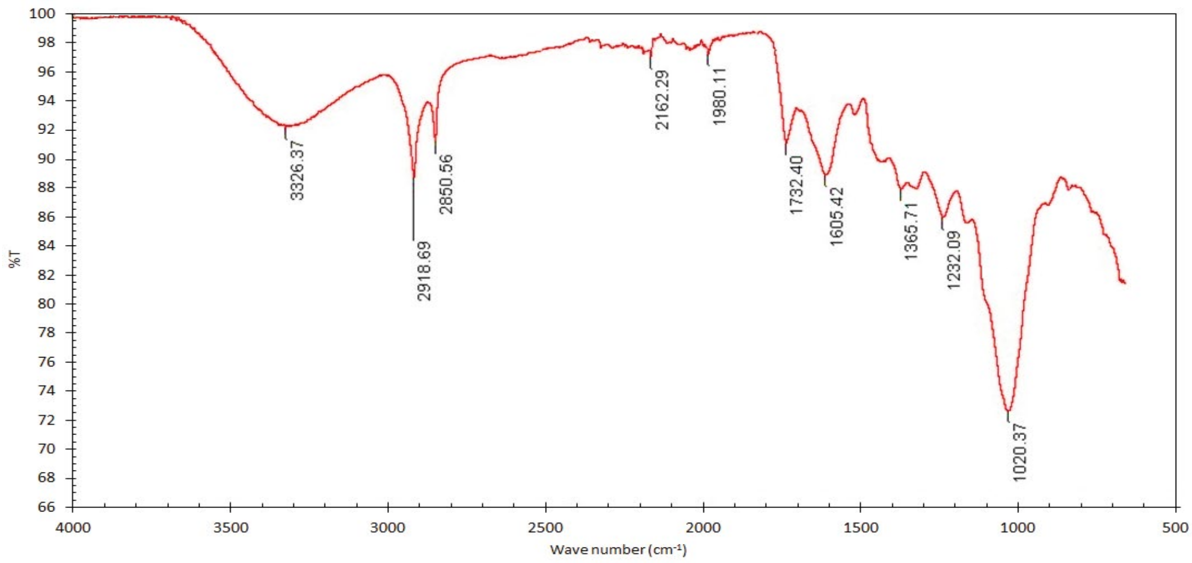

Fig. 1. FT-IR spectrum of the acid-treated material.

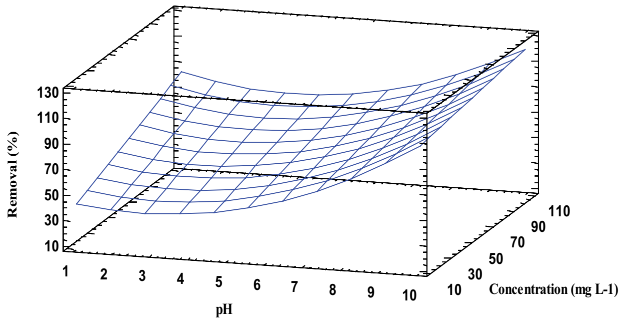

Fig. 2. 3D plot: interactive effect of pH and concentration on the removal of Ni(II) ions.

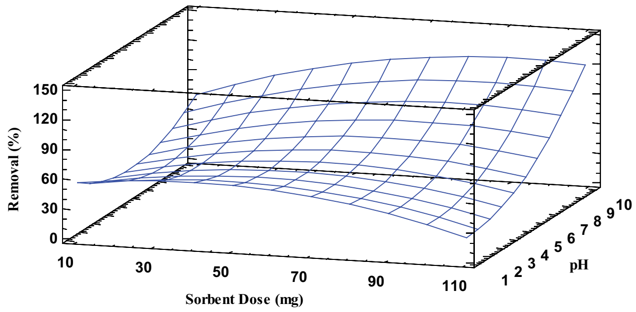

Fig. 3. 3D plot: interactive effect of sorbent dose and pH on Ni(II) ions removal.

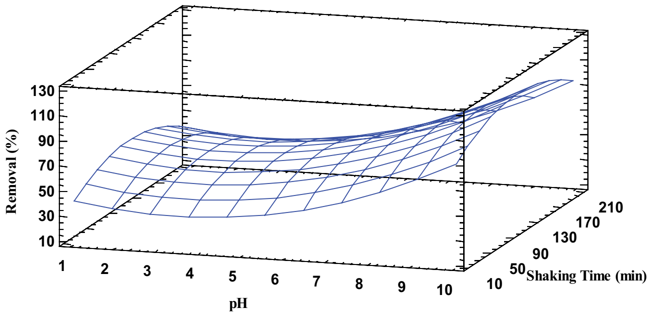

Fig. 4. 3D plot: interactive effect of pH and shaking time on Ni(II) ions removal.

optimum level of pH 8 and time 90 min. The result shows that the removal was increased with an increase in adsorbent dose 10–60 mg, remained almost constant with further increase in adsorbent dose 60–100 mg as system attained the equilibrium, while removal was also increased with increase in the concentration of Ni(II) ions.

3.2.6. Effect of concentration and shaking time

Fig. 7 shows the interactive effect of concentration ranging 10–100 mg L^{-1} and shaking time ranging 10–180 min on the removal of Ni(II) ions at the optimum level of pH 8 and sorbent dose 70 mg. The result shows that the removal was increased with increase in shaking time until equilibrium was attained at 90 min and remained almost constant with further increase in shaking time as system attained the equilibrium, while concentration has almost same effect as discussed in subsection 3.2.1.

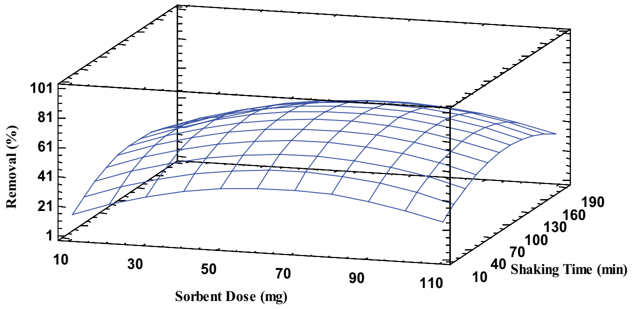

Fig. 5. 3D plot: interactive effect of shaking time and sorbent dose on Ni(II) ions removal.

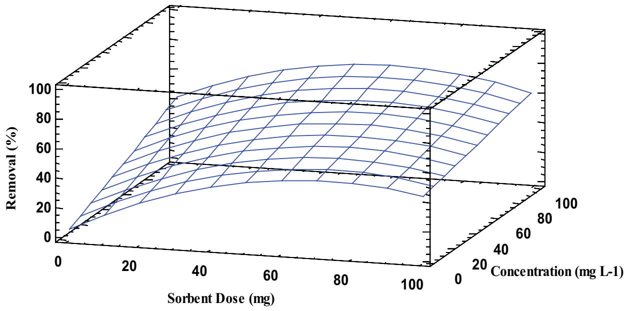

Fig. 6. 3D plot: interactive effect of concentration and adsorbent dose on Ni(II) ions removal

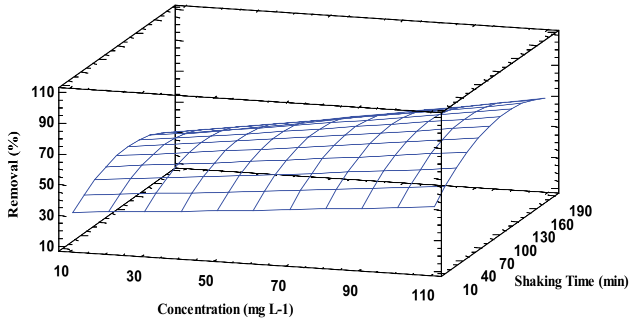

Fig. 7. 3D plot: interactive effect of concentration and shaking time on Ni(II) ions removal.

3.3. Main effects plot

Fig. 8 depicts the main effect plot, which shows the effect of four factors individually on the removal of Ni(II) ions keeping the other three factors at their optimum levels. The main effect plot shows that the removal was increased with increase of adsorbent dose and decreased with further increase of adsorbent dose. The removal was increased with increase of shaking time and decreased with further increase of shaking time due to the desorption. The effect of pH is depicted as removal was slightly changed in the

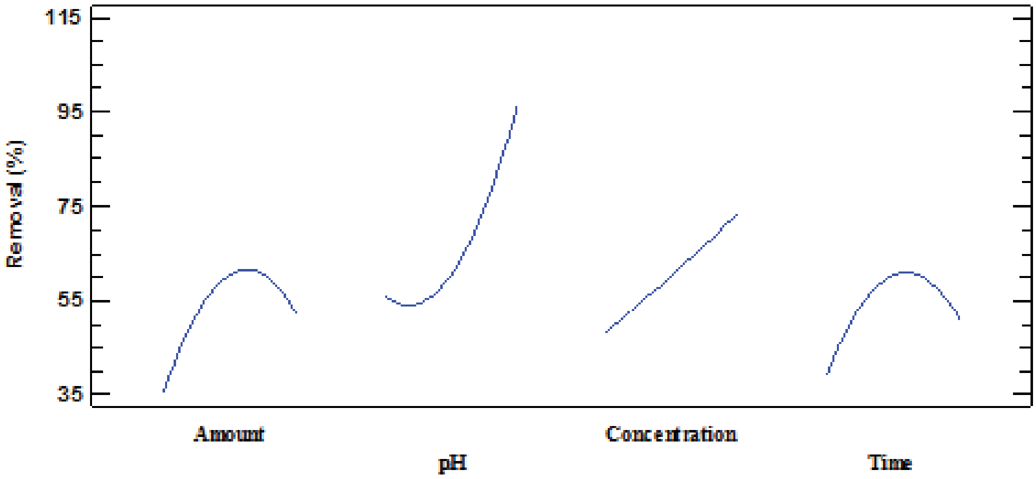

Fig. 8. Main effect plot for Ni(II) ions removal.

beginning and sharply increased with further increase in pH. The removal also increased linearly with the increase of concentration. The removal was sharply increased and declined with increase of adsorbent dose. The shaking time and has same effect as adsorbent dose.

3.4. Analysis of variance

The fitting and accuracy of the CCD model was evaluated by analysis of variance. Model fitting and significance of factors can be predicted from the numerical values of *P* and *F*. The model is said to be well fitted to experimental data if $P < 0.05$ and the higher numerical value of *F* [20,21]. Table 3 shows that the numerical value of *P* is less than 0.05 for all effects except *AD*, which indicated that all the null hypotheses are rejected except *AD*. Therefore, all the experimental data except *AD* are significant. The numerical values of regression coefficients are positive for all effects except *AD*, which indicated that adsorption was increased with increasing the factors except *AD*.

3.5. Effect of matrix ions

The sensitivity and selectivity of the adsorbent were highly influenced by matrix ions. Therefore, the effect of matrix ions such as CH_3COO^-, CO_3^{2-}, SO_4^{2-}, F^-, PO_4^{3-}, NO_3^-, Ca^{2+}, HCO_3^-, Na^+, K^+, Ba^{2+} and Mg^{2+} was studied for the Ni(II) ions adsorption. The matrix ions were fixed in 1:10 ratio and Ni(II) ions adsorption was adsorbed ≥95.0%, and in presence of heavy metal ions such as Pb(II), Cu(II), Zn(II) and Cd(II) ions in the ratio of 1:1, the removal of Ni(II) ions was achieved ≥94.0%, which indicated that adsorbent possessed high tolerance for matrix ions.

3.6. Adsorption mechanism

The proportion of Ni(II) ions species in aqueous solution is strongly pH-dependent. At pH 4–8, Ni^{2+} exists as the main species. At pH > 8, Ni(II) ions started to form precipitates of hydroxides such as $Ni(OH)_4^{2-}$, $Ni(OH)_3^-$, $Ni(OH)_2$ and $Ni(OH)^+$ [22]. The adsorbent contained different functionalities such as carboxylic acid (R–COOH), alcohol (R–OH) and phenol (Ar–OH). At pH 8, the adsorbent became negatively charged due to the deprotonation of R–COOH, R–OH and Ar–OH moieties which interacted with Ni^{2+} during adsorption [23].

Table 3
Analysis of variance

Factors	*F*-Ratio	*P*-Value	Regression coefficient
A: Amount	128.28	0.0015	0.001
B: pH	705.47	0.0001	12.337
C: Concentration	1,406.82	0.0010	0.430
D: Time	60.93	0.0044	0.182
AB	312.99	0.0004	0.095
AC	112.82	0.0018	0.001
AD	0.04	0.8506	–0.004
BC	158.09	0.0011	0.030
BD	2.77	0.0194	0.004
CD	124.98	0.0015	0.001

3.7. Equilibrium studies

3.7.1. Langmuir

This model is based on the assumption that all the active sites of adsorbent are structurally identical and energetically equivalent. Adsorption takes place at homogeneously distributed sites onto the surface of adsorbent without interaction between adsorbed ions or molecules [24,25]. The Langmuir isotherm was plotted by varying the concentration of Ni(II) ions while other factors were kept constant at their optimum levels such as adsorbent dose = 70 mg, pH 8, shaking time = 95 min at 25°C. The linear form of Langmuir isotherm is represented by Eq. (2) [26]. The characteristic of Langmuir isotherm is the separation factor (R_L), which can be calculated by Eq. (3). The numerical value of R_L indicates the feasibility of adsorption. The adsorption may be irreversible ($R_L = 0$), unfavorable ($R_L > 1$) and favorable ($0 < R_L < 1$) [27].

$$\frac{C_e}{C_{\text{ads.}}} = \frac{1}{Q}C_e + \frac{1}{Qb_L} \tag{2}$$

$$R_L = \frac{1}{1+\left(b_L C_i\right)} \tag{3}$$

where C_e (mg L^{-1}) is the concentration of adsorbate in solution, $C_{\text{ads.}}$ (mg g^{-1}) is the concentration of adsorbate onto the surface of adsorbent at the equilibrium stage and C_i (mg L^{-1}) is the initial concentration of adsorbate. Q is the monolayer coverage and b_L (L mg^{-1}) is the Langmuir constant related to the binding energy of solute, respectively. The Langmuir isotherm was plotted as $C_e/C_{\text{ads.}}$ vs. C_e. The isotherm fitted well to experimental data with R^2 of 0.995. The monolayer sorption capacity of adsorbent was found to be 45.3 ± 2.4 mg g^{-1}. The numerical values of R_L values calculated were calculated and found to be in the range of 0.002–0.07, which indicated that the adsorption of Ni(II) ions was favorable.

3.7.2. Dubinin–Radushkevich isotherm

The Dubinin–Radushkevich (D–R) isotherm assumes no homogeneous surface of the adsorbent material. It is useful to estimate the characteristics porosity of the adsorbent and apparent free energy of adsorption The linear form of D–R isotherm is represented by Eq. (4) [28].

$$\ln C_{\text{ads}} = \ln K_{(D-R)} - \beta\varepsilon^2 \tag{4}$$

$$\varepsilon = RT \ln\left(1+\frac{1}{C_e}\right) \tag{5}$$

$$E = \frac{1}{\sqrt{-2\beta}} \tag{6}$$

where $C_{\text{ads.}}$ (mg g^{-1}) is the amount adsorbate adsorbed onto the adsorbent at equilibrium, β is the slope of D–R isotherm, $K_{\text{D–R}}$ is D–R constant, and ε is Polanyi potential, which can be calculated using Eq. (5). R is the general gas constant, T is temperature and E is sorption energy, which can be calculated using Eq. (6). The adsorption may be physisorption if $E < 8$ kJ mol^{-1} or chemisorption if $E > 8$–16 kJ mol^{-1} [29]. D–R isotherm was plotted as $\ln C_{\text{ads.}}$ vs. ε^2 The plot fitted well with R^2 of 0.989. The E was calculated and found to be 14.81 ± 1.5 kJ mol^{-1}, indicated adsorption of Ni(II) ions proceeded via chemisorption or ion exchange.

4. Application of the method

The repeatability of the developed method was checked by applying on real and spiked water samples. Ni(II) ions uptake from the samples was achieved ≥ 91.0% as shown in Table 4. The result shows that sample collected from the industrial area was Ni(II) ions contaminated.

5. Comparison with reported bio-sorbents

Different methods have been developed for the removal of Ni(II) ions from environmental water samples using different bio-sorbents. In this method, strawberry calyx waste-based adsorbent was used for the adsorption of Ni(II) ions. The capacity of this adsorbent for the uptake of Ni(II) ions was found comparatively better than the reported bio-sorbents as shown in Table 5.

Table 4
Application of method: removal of Ni(II) ions from spiked real water samples

Sample	Added value (mg L^{-1})	Found value (mg L^{-1})	Removal (%)
Tap water	0	Not detected	–
	5	4.8	96.0
	10	9.7	97.0
	20	19.8	95.0
Tap water	0	Not detected	–
	5	4.9	99.0
	10	9.5	95.0
	20	18.5	94.2
Waste water (CETP, Korangi)	0	6.8	91.0
	5	11.6	98.0
	10	16.4	97.0
	20	26.0	98.5

Table 5
Comparative capacities of different bio-sorbents for Ni(II) ions adsorption

Adsorbent	pH	Capacity (mg g^{-1})	Reference
Cashew nut shell	5.0	18.9	[29]
Pine cone treated with HCl	8.0	1.7	[30]
Pine bark treated with HCl	8.0	20.6	[30]
Husk of *Lathyrus sativus*	5.0	15.7	[31]
Oak sawdust trsted with HCl	80	3.4	[32]
Hazelnut shell activated carbon	3.0	8.5	[33]
Moringa oleifera bark	6.0	30.3	[34]
Coconut copra meal	6.0	3.8	[35]
Grape stalks wastes	6.0	106.7	[36]
Black carrot residue	5.2	6.5	[37]
Barley straw	4.8	35.8	[38]
Rice bran treated with H_3PO_4	6.0	102.0	[39]
Orange peel	5.5	9.8	[40]
Mango peel	5.0	39.8	[41]
Strawberry calyx waste	8.0	45.3 ± 2.4	[Present method]

6. Conclusion

Pretreated strawberry calyx waste material was used for the adsorption of Ni(II) ions and removal was 45%. The performance of the material was enhanced by treating with HCl and the removal was increased to 98.5% with RSD ≤ 3.5% at optimum conditions. HCl treated strawberry calyx waste adsorbent worked well for the adsorption of Ni(II) ions at pH 8 due to the presence of hydroxyl (–OH) groups of alcohol and carboxylic acid. The studied adsorbent was recycled 10 times without significant loss (1%–5%) in uptake capacity. The adsorbent was found pH-sensitive which indicated the presence of polar functional groups onto the adsorbent. The adsorption could take place through chemisorption or ion exchange in basic medium. Multivariate sorption optimization was carried out by the CCD model. The numerical value of P is less than 0.05 for all effects except adsorbent dose and shaking time which indicated that all the null hypotheses are rejected except the interactive effect of adsorbent dose and shaking time. Langmuir and D–R isotherms fitted well to adsorption data with R^2 of 0.995 and 0.989, respectively.

Acknowledgments

Authors would like to thank Professor Dr. Murat Sari, Department of Mathematics, Yildiz Technical University, Istanbul-Turkey for his scientific guidance in central composite design development and statistical analyses. Authors also like to thank the Institute of Advance Research Studies in Chemical Science, University of Sindh, Jamshoro 76080, Pakistan for providing instrumental facilities throughout this research.

References

[1] A. Imran, New generation adsorbents for water treatment, Chem. Rev., 112 (2012) 5073–5091.

[2] R.R.V. Hemavathy, P.S. Kumar, S. Suganya, V. Swetha, S.J. Varjani, Modelling on the removal of toxic metal ions from aquatic system by different surface modified *Cassia fistula* seeds, Bioresour. Technol., 281 (2019) 1–9.

[3] A.I. Mohammed, S.G. Gupta, Studies on heavy metal ion pollution of ground water sources as an effect of municipal solid waste dumping, Afr. J. Basic Appl. Sci., 1 (2009) 117–122.

[4] R.T. Nickson, J.M. McArthur, B. Shrestha, T.O. Kyaw-Myint, D. Lowry, Arsenic and other drinking water quality issues, Muzaffargarh District, Pakistan, Appl. Geochem., 20 (2005) 55–68.

[5] A.K. Tonni, E.T.S. Mika, S. Markus, Nanoadsorbents for remediation of aquatic environment: Local and practical solutions for global water pollution problems, Crit. Rev. Env. Sci. Technol., 42 (2012) 1233–1295.

[6] J. Lesley, J. Byung-Moon, R.V.F. Joseph, M.P. Chang, Y. Yeomin, Removal of heavy metals from water sources in the developing world using low-cost materials: a review, Chemosphere, 229 (2019) 142–159.

[7] I. Anastopoulos, I. Pashalidis, A. Hosseini-Bandegharaei, D.A. Giannakoudakis, A. Robalds, M. Usman, L.B. Escudero, Y. Zhou, J.C. Colmenares, A. Nunez-Delgado, E.C. Lima, Agricultural biomass/waste as adsorbents for toxic metal decontamination of aqueous solutions, J. Mol. Liq., 295 (2019) 111684.

[8] I. Aminul, A. Ahmad, A.L. Mohammad, Characterization of a chelating resin functionalized via azo spacer and its analytical applicability for the determination of trace metal ions in real matrices, J. Appl. Polym. Sci., 123 (2012) 3448–3458.

[9] M.R. Awual, M.M. Hasan, Colorimetric detection and removal of copper(II) ions from wastewater samples using tailor-made composite adsorbent, Sens. Actuators B, 206 (2015) 692–700.

[10] M.A. Momodu, C.A. Anyakora, Heavy metal contamination of ground water: the surulere case study, Res. J. Environ. Earth Sci., 2 (2010) 39–43.

[11] S. Ahmet, T. Mustafa, C. Demirhan, S. Mustafa, Equilibrium, kinetic and thermodynamic studies of adsorption of Pb(II) from aqueous solution onto Turkish kaolinite clay, J. Hazard. Mater., 149 (2007) 283–291.

[12] M. Emine, N. Yasar, Investigations of nickel(II) removal from aqueous solutions using tea factory waste, J. Hazard. Mater., 127 (2005) 120–128.

[13] H. Halil, Adsorption of nickel(II) from aqueous solution onto activated carbon prepared from almond husk, J. Hazard. Mater., 97 (2003) 49–57.

[14] A.K. Meena, G.K. Mishra, P.K. Rai, C. Rajagopal, P.N. Nagar, Removal of heavy metal ions from aqueous solutions using carbon aerogel as an adsorbent, J. Hazard. Mater., 122 (2005) 161–170.

[15] A. Bhatnagar, M. Sillanpaa, Utilization of agro-industrial and municipal waste materials as potential adsorbents for water treatment-a review, Chem. Eng. J., 157 (2010) 277–296.

[16] M.R. Awual, G.E. Eldesoky, T. Yaita, Mu. Naushad, H. Shiwaku, Z.A. AlOthman, S. Suzuki, Schiff based ligand containing nanocomposite adsorbent for optical copper(II) ions removal from aqueous solutions, Chem. Eng. J., 279 (2015) 639–647.

[17] A. Demirbas, Heavy metal adsorption onto agro-based waste materials: a review, J. Hazard. Mater., 157 (2008) 220–229.

[18] H. Karl, P. Klaus, New versus old scientific names in strawberries (*Fragaria L.*), Genet. Resour. Crop Evol., 50 (2003) 789–791.

[19] A.N. Siyal, S.Q. Memon, M.I. Khaskheli, Optimization and equilibrium studies of Pb(II) removal by Grewia Asiatica seed: a factorial design approach, Pol. J. Chem. Technol., 14 (2012) 71–77.

[20] S.H. Hasan, P. Srivastav, M. Talat, Biosorption of Pb(II) from water using biomass of *Aeromonas hydrophila*: central composite design for optimization of process variables, J. Hazard. Mater., 168 (2009) 1155–1162.

[21] M.M.D. Zulkali, A.L. Ahmad, N.H. Norulakmal, *Oryza sativa L.* husk as heavy metal adsorbent: optimization with lead as model solution, Bioresour. Technol., 97 (2006) 21–25.

[22] G. Sheng, S. Yang, J. Sheng, D. Zhao, X. Wang, Influence of solution chemistry on the removal of Ni(II) from aqueous solution to titanate nanotubes, Chem. Eng. J., 168 (2011) 178–182.

[23] W. Yunhai, W. Yajun, Z. Jianxin, C. Julin, J. Yanping, W. Yunying, Comparative and competitive adsorption of Cr(VI), As(III), and Ni(II) onto coconut charcoal, Environ. Sci. Pollut. Res. Int., 20 (2013) 2210–2219.

[24] F. Gimbert, N. Morin-Crini, R. Francois, B. Pierre-Marie, C. Gregorio, Adsorption isotherm models for dye removal by cationized starch-based material in a single component system: error analysis, J. Hazard. Mater., 157 (2008) 34–46.

[25] M.R. Awual, Solid phase sensitive palladium(II) ions detection and recovery using ligand based efficient conjugate nanomaterials, Chem. Eng. J., 300 (2016) 264–272.

[26] M.R. Awual, M.M. Hasan, M.A. Khaleque, Efficient selenium(IV) detection and removal from water by tailor-made novel conjugate adsorbent, Sens. Actuators, B, 209 (2015) 194–202.

[27] S.Q. Memon, S.M. Hasany, M.I. Bhanger, M.Y. Khuhawar, Enrichment of Pb(II) ions using phthalic acid functionalized XAD-16 resin as a sorbent, J. Colloid Interface Sci., 291 (2005) 84–91.

[28] S.M. Hasany, M.H. Chaudhary, Sorption potential of Hare River sand for the removal of antimony from acidic aqueous solution, Appl. Radiat. Isot., 47 (1996) 467–471.

[29] P.S. Kumar, S. Ramalingam, S.D. Kirupha, A. Murugesan, T. Vidhyadevi, S. Sivanesan, Adsorption behavior of nickel(II) onto cashew nut shell: equilibrium, thermodynamics, kinetics, mechanism and process design, Chem. Eng. J., 167 (2011) 122–131.

[30] M.E. Argun, S. Dursun, K. Gur, C. Ozdemir, M. Karatas, S. Dogan, Nickel adsorption on the modified pine tree materials, Environ. Technol., 26 (2005) 479–488.

[31] G.C. Panda, S.K. Das, T.S. Bandopadhyay, A.K. Guha, Adsorption of nickel on husk of *Lathyrus sativus*: behavior and binding mechanism, Colloids Surf. B Biointerfaces, 57 (2007) 135–142.

[32] M.E. Argun, S. Dursun, C. Ozdemir, M. Karatas, Heavy metal adsorption by modified oak sawdust: thermodynamics and kinetics, J. Hazard. Mater., 141 (2007) 77–85.

[33] E. Demirbas, M. Kobya, S. Oncel, S. Sencan, Removal of Ni(II) from aqueous solution by adsorption onto hazelnut shell activated carbon: equilibrium studies, Bioresour. Technol., 84 (2002) 291–293.

[34] D.H.K. Reddy, D.K.V. Ramana, K. Seshaiah, A.V.R. Reddy, Biosorption of Ni(II) from aqueous phase by *Moringa oleifera* bark, a low cost biosorbent, Desalination, 268 (2011) 150–157.

[35] M. Saleem, N. Wongsrisujarit, S. Boonyarattanakalin, Removal of nickel (II) ion by adsorption on coconut copra meal biosorbent, Desal. Water Treat., 57 (2016) 5623–5635.

[36] I. Villaescusa, N. Fiol, M. Martínez, N. Miralles, J. Poch, J. Serarols, Removal of copper and nickel ions from aqueous solutions by grape stalks wastes, Water Res., 38 (2004) 992–1002.

[37] F. Güzel, H. Yakut, G. Topal, Determination of kinetic and equilibrium parameters of the batch adsorption of Mn(II), Co(II), Ni(II) and Cu(II) from aqueous solution by black carrot (*Daucus carota L.*) residues, J. Hazard. Mater., 153 (2008) 1275–1287.

[38] A. Thevannan, R. Mungroo, C.H. Niu, Biosorption of nickel with barley straw, Bioresour. Technol., 101 (2010) 1776–1780.

[39] M.N. Zafar, R. Nadeemb, M.A. Hanif, Biosorption of nickel from protonated rice bran, J. Hazard. Mater., 143 (2007) 478–485.

[40] N. Feng, X. Guo, S. Liang, Y. Zhu, J. Liu, Biosorption of heavy metals from aqueous solutions by chemically modified orange peel, J. Hazard. Mater., 18 (2011) 49–54.

[41] M. Iqbal, A. Saeed, I. Kalim, Characterization of adsorptive capacity and investigation of mechanism of Cu^{2+}, Ni^{2+} and Zn^{2+} adsorption on mango peel waste from constituted metal solution and genuine electroplating effluent, Sep. Sci. Technol., 44 (2009) 3770–3791.